

CLNS 97/1485
CLEO 97-11

A New Measurement of $B \rightarrow D^* \pi$ Branching Fractions

CLEO Collaboration

(November 22, 2018)

Abstract

The unique kinematics of $B\bar{B}$ production at the $\Upsilon(4S)$ allow reconstruction of all kinematic quantities in the decay sequence $B \rightarrow D^* \pi$, $D^* \rightarrow D\pi$ without reconstructing the D decay. Using 3.1 fb^{-1} accumulated at the $\Upsilon(4S)$ by the CLEO-II detector, we report measurements of $\mathcal{B}(\bar{B}^0 \rightarrow D^{*+} \pi^-) = (2.81 \pm 0.11 \pm 0.21 \pm 0.05) \times 10^{-3}$ and $\mathcal{B}(B^- \rightarrow D^{*0} \pi^-) = (4.34 \pm 0.33 \pm 0.34 \pm 0.18) \times 10^{-3}$.

G. Brandenburg,¹ R. A. Briere,¹ Y. S. Gao,¹ D. Y.-J. Kim,¹ R. Wilson,¹ H. Yamamoto,¹
 T. E. Browder,² F. Li,² Y. Li,² J. L. Rodriguez,² T. Bergfeld,³ B. I. Eisenstein,³ J. Ernst,³
 G. E. Gladding,³ G. D. Gollin,³ R. M. Hans,³ E. Johnson,³ I. Karliner,³ M. A. Marsh,³
 M. Palmer,³ M. Selen,³ J. J. Thaler,³ K. W. Edwards,⁴ A. Bellerive,⁵ R. Janicek,⁵
 D. B. MacFarlane,⁵ K. W. McLean,⁵ P. M. Patel,⁵ A. J. Sadoff,⁶ R. Ammar,⁷ P. Baringer,⁷
 A. Bean,⁷ D. Besson,⁷ D. Coppage,⁷ C. Darling,⁷ R. Davis,⁷ N. Hancock,⁷ S. Kotov,⁷
 I. Kravchenko,⁷ N. Kwak,⁷ S. Anderson,⁸ Y. Kubota,⁸ M. Lattery,⁸ S. J. Lee,⁸
 J. J. O'Neill,⁸ S. Patton,⁸ R. Poling,⁸ T. Riehle,⁸ V. Savinov,⁸ A. Smith,⁸ M. S. Alam,⁹
 S. B. Athar,⁹ Z. Ling,⁹ A. H. Mahmood,⁹ H. Severini,⁹ S. Timm,⁹ F. Wappler,⁹
 A. Anastassov,¹⁰ S. Blinov,^{10,*} J. E. Duboscq,¹⁰ K. D. Fisher,¹⁰ D. Fujino,^{10,†} R. Fulton,¹⁰
 K. K. Gan,¹⁰ T. Hart,¹⁰ K. Honscheid,¹⁰ H. Kagan,¹⁰ R. Kass,¹⁰ J. Lee,¹⁰ M. B. Spencer,¹⁰
 M. Sung,¹⁰ A. Undrus,^{10,*} R. Wanke,¹⁰ A. Wolf,¹⁰ M. M. Zoeller,¹⁰ B. Nemati,¹¹
 S. J. Richichi,¹¹ W. R. Ross,¹¹ P. Skubic,¹¹ M. Wood,¹¹ M. Bishai,¹² J. Fast,¹² E. Gerndt,¹²
 J. W. Hinson,¹² N. Menon,¹² D. H. Miller,¹² E. I. Shibata,¹² I. P. J. Shipsey,¹² M. Yurko,¹²
 L. Gibbons,¹³ S. D. Johnson,¹³ Y. Kwon,¹³ S. Roberts,¹³ E. H. Thorndike,¹³ C. P. Jessop,¹⁴
 K. Lingel,¹⁴ H. Marsiske,¹⁴ M. L. Perl,¹⁴ S. F. Schaffner,¹⁴ D. Ugolini,¹⁴ R. Wang,¹⁴
 X. Zhou,¹⁴ T. E. Coan,¹⁵ V. Fadeyev,¹⁵ I. Korolkov,¹⁵ Y. Maravin,¹⁵ I. Narsky,¹⁵
 V. Shelkov,¹⁵ J. Staeck,¹⁵ R. Stroynowski,¹⁵ I. Volobouev,¹⁵ J. Ye,¹⁵ M. Artuso,¹⁶
 A. Efimov,¹⁶ F. Frasconi,¹⁶ M. Gao,¹⁶ M. Goldberg,¹⁶ D. He,¹⁶ S. Kopp,¹⁶ G. C. Moneti,¹⁶
 R. Mountain,¹⁶ S. Schuh,¹⁶ T. Skwarnicki,¹⁶ S. Stone,¹⁶ G. Viehhauser,¹⁶ X. Xing,¹⁶
 J. Bartelt,¹⁷ S. E. Csorna,¹⁷ V. Jain,¹⁷ S. Marka,¹⁷ A. Freyberger,¹⁸ R. Godang,¹⁸
 K. Kinoshita,¹⁸ I. C. Lai,¹⁸ P. Pomianowski,¹⁸ S. Schrenk,¹⁸ G. Bonvicini,¹⁹ D. Cinabro,¹⁹
 R. Greene,¹⁹ L. P. Perera,¹⁹ G. J. Zhou,¹⁹ B. Barish,²⁰ M. Chadha,²⁰ S. Chan,²⁰ G. Eigen,²⁰
 J. S. Miller,²⁰ C. O'Grady,²⁰ M. Schmidtler,²⁰ J. Urheim,²⁰ A. J. Weinstein,²⁰
 F. Würthwein,²⁰ D. M. Asner,²¹ D. W. Bliss,²¹ W. S. Brower,²¹ G. Masek,²¹ H. P. Paar,²¹
 V. Sharma,²¹ J. Gronberg,²² T. S. Hill,²² R. Kutschke,²² D. J. Lange,²² S. Menary,²²
 R. J. Morrison,²² H. N. Nelson,²² T. K. Nelson,²² C. Qiao,²² J. D. Richman,²² D. Roberts,²²
 A. Ryd,²² M. S. Witherell,²² R. Balest,²³ B. H. Behrens,²³ K. Cho,²³ W. T. Ford,²³
 H. Park,²³ P. Rankin,²³ J. Roy,²³ J. G. Smith,²³ J. P. Alexander,²⁴ C. Bebek,²⁴
 B. E. Berger,²⁴ K. Berkelman,²⁴ K. Bloom,²⁴ D. G. Cassel,²⁴ H. A. Cho,²⁴
 D. M. Coffman,²⁴ D. S. Crowcroft,²⁴ M. Dickson,²⁴ P. S. Drell,²⁴ K. M. Ecklund,²⁴
 R. Ehrlich,²⁴ R. Elia,²⁴ A. D. Foland,²⁴ P. Gaidarev,²⁴ B. Gittelman,²⁴ S. W. Gray,²⁴
 D. L. Hartill,²⁴ B. K. Heltsley,²⁴ P. I. Hopman,²⁴ J. Kandaswamy,²⁴ N. Katayama,²⁴
 P. C. Kim,²⁴ D. L. Kreinick,²⁴ T. Lee,²⁴ Y. Liu,²⁴ G. S. Ludwig,²⁴ J. Masui,²⁴
 J. Mevissen,²⁴ N. B. Mistry,²⁴ C. R. Ng,²⁴ E. Nordberg,²⁴ M. Ogg,^{24,‡} J. R. Patterson,²⁴
 D. Peterson,²⁴ D. Riley,²⁴ A. Soffer,²⁴ C. Ward,²⁴ M. Athanas,²⁵ P. Avery,²⁵ C. D. Jones,²⁵
 M. Lohner,²⁵ C. Prescott,²⁵ J. Yelton,²⁵ and J. Zheng²⁵

*Permanent address: BINP, RU-630090 Novosibirsk, Russia.

†Permanent address: Lawrence Livermore National Laboratory, Livermore, CA 94551.

‡Permanent address: University of Texas, Austin TX 78712

¹Harvard University, Cambridge, Massachusetts 02138
²University of Hawaii at Manoa, Honolulu, Hawaii 96822
³University of Illinois, Champaign-Urbana, Illinois 61801
⁴Carleton University, Ottawa, Ontario, Canada K1S 5B6
and the Institute of Particle Physics, Canada
⁵McGill University, Montréal, Québec, Canada H3A 2T8
and the Institute of Particle Physics, Canada
⁶Ithaca College, Ithaca, New York 14850
⁷University of Kansas, Lawrence, Kansas 66045
⁸University of Minnesota, Minneapolis, Minnesota 55455
⁹State University of New York at Albany, Albany, New York 12222
¹⁰Ohio State University, Columbus, Ohio 43210
¹¹University of Oklahoma, Norman, Oklahoma 73019
¹²Purdue University, West Lafayette, Indiana 47907
¹³University of Rochester, Rochester, New York 14627
¹⁴Stanford Linear Accelerator Center, Stanford University, Stanford, California 94309
¹⁵Southern Methodist University, Dallas, Texas 75275
¹⁶Syracuse University, Syracuse, New York 13244
¹⁷Vanderbilt University, Nashville, Tennessee 37235
¹⁸Virginia Polytechnic Institute and State University, Blacksburg, Virginia 24061
¹⁹Wayne State University, Detroit, Michigan 48202
²⁰California Institute of Technology, Pasadena, California 91125
²¹University of California, San Diego, La Jolla, California 92093
²²University of California, Santa Barbara, California 93106
²³University of Colorado, Boulder, Colorado 80309-0390
²⁴Cornell University, Ithaca, New York 14853
²⁵University of Florida, Gainesville, Florida 32611

The factorization hypothesis asserts [1] that hadronic two body decays of B mesons can be expressed as the product of two independent hadronic currents, in analogy to semileptonic decays. For the external spectator decays, in which the W hadronizes into a single meson, this is expected to be a good approximation. For internal color-suppressed decays the validity of this assumption is unknown. The phenomenological Hamiltonian adopted by Bauer, Stech and Wirbel [2] is an approach in which the Hamiltonian is the product of the CKM matrix elements, the hadronic currents, and correction coefficients for hard gluon exchange: a_1 for external spectator diagrams and a_2 for the internal color-suppressed diagrams. In the absence of final state QCD interactions a_1 is expected to be one, while a_2 is not known *a priori*. The Cabibbo-favored decay $B^- \rightarrow D^{*0}\pi^-$ proceeds through both external spectator and internal color-suppressed diagrams, while $\bar{B}^0 \rightarrow D^{*+}\pi^-$ proceeds only through the external spectator diagram. A measurement of the ratio of these two decays thus determines a_2/a_1 . This ratio could then be used to predict the rate of the color-suppressed decay $\bar{B}^0 \rightarrow D^{*0}\pi^0$, which proceeds only through the internal color-suppressed diagram.

Both CLEO [3] and ARGUS [4] have reported measurements of these decays based on the full reconstruction of all final state particles. Reconstructing only the fast pion (π_f) from the B decay and the slow pion (π_s) from the D^* decay, however, increases signal acceptance by an order of magnitude and removes systematic uncertainties from the D reconstruction. Previous partial-reconstruction techniques [5] have used the two pions to construct the B mass. In contrast, the current technique assumes the nominal B mass as an input. This allows all of the degrees of freedom of the decay to be determined up to a quadratic ambiguity.

The $B \rightarrow D^*\pi_f$, $D^* \rightarrow D\pi_s$ decay chain is reconstructed by measuring the 4-vectors of the 2 pions without measuring the D 4-vector. We can then require that there exist a D 4-vector able to simultaneously satisfy energy-momentum conservation in both the B and D^* decays. Energy-momentum conservation in the B (D^*) decay defines a cone of possible D^* 4-vectors around the π_f (π_s) direction. We use the D^* 4-vector rather than the D 4-vector since it simplifies the calculations. These two cones must overlap for there to be a simultaneous solution. In order to define these two cones we must assume the B, D^* , and D masses and constrain the B energy to be the beam energy.

The measurement of the two pions gives 3 significant quantities, the momentum of each pion, $|P_{\pi_f}|$ and $|P_{\pi_s}|$, and the angle between them, α . We use these quantities to construct the two cones, using the following procedure. We determine the D^* energy and momentum by requiring energy conservation in the B decay, $E_{D^*} = E_B - E_{\pi_f}$ and $|P_{D^*}| = (E_{D^*}^2 - m_{D^*}^2)^{0.5}$. Then applying momentum conservation we require the B momentum vector to be equal to the sum of the D^* and π_f momentum vectors. The three vectors form a triangle which defines the angle, γ , between the π_f and the D^* . The possible solutions for the D^* momentum vector are then constrained to lie on a cone around the π_f direction with an opening angle of γ . For some values of the π_f momentum the triangle will not close; these values have no possible solution. In such cases, γ is defined to be zero. The analogous procedure is followed in the D^* decay to determine D energy and momentum. Forming a triangle from the D^* , D and π_s momentum vectors determines the angle, β , between the D^* and the π_s . The D^* momentum vector is then constrained to lie on a cone around the π_s direction with an opening angle of β .

The final requirement for the two pions to be consistent with $B \rightarrow D^*\pi$ production is that

the two cones overlap. The opening angles of the cones determines the range of values of α , the angle between the pions, for which an overlap can occur. The value of $\cos \alpha$ must fall within a region whose width, w , and center, c , are defined by $\sin \gamma \times \sin \beta$ and $\cos \gamma \times \cos \beta$ respectively. When the equation $|\cos \alpha - c| < w$ is satisfied the cones overlap.

Once the decay is reconstructed two quantities of physical interest can be constructed, $\cos \theta_B^*$, the π_f direction relative to the B boost direction in the B center of mass and $\cos \theta_{D^*}^*$, the π_s direction relative to the D^* boost direction in the D^* center of mass. In the decay $B \rightarrow D^* \pi$, angular momentum conservation dictates that the D^* be produced with zero helicity. The distribution of signal events in $\cos \theta_{D^*}^*$ is therefore expected to be proportional to $\cos^2 \theta_{D^*}^*$. In $\cos \theta_B^*$ the distribution of signal events is expected to be flat because the B is a pseudoscalar. In both cases signal events must lie between ± 1 .

The two quantities $\cos \theta_B^*$ and $\cos \theta_{D^*}^*$ are proportional to $|P_{\pi_f}|$ and $|P_{\pi_s}|$ respectively. Therefore the signal distributions will be smeared by any pion momentum mismeasurements. The cone opening angles γ and β , however, depend non-linearly on the pion momenta, diverging when the opening angle is zero. Since the quantity w depends on the sines of these opening angles we loosen the requirement on $\cos \alpha$ by requiring $|\cos \alpha - c| < w + 0.02$. This leads to a finite acceptance for events outside the signal region.

The two pion candidates are classified according to their charge. Signal events always have a charged fast pion, but the slow pion can be either charged ($\pi_f^- \pi_s^+$) or neutral ($\pi_f^- \pi_s^0$). Neutral slow pions are produced both from D^{*0} and $D^{*\pm}$ decays but charged slow pions are only produced in $D^{*\pm}$ decays. Therefore $\pi_f^- \pi_s^0$ events will contain contributions from both $\overline{B}^0 \rightarrow D^{*+} \pi^-$ and $B^- \rightarrow D^{*0} \pi^-$, but $\pi_f^- \pi_s^+$ events will contain only $\overline{B}^0 \rightarrow D^{*+} \pi^-$ decays.

The data used in this analysis were selected from hadronic events produced in e^+e^- annihilations at the Cornell Electron Storage Ring (CESR). The data sample consists of 3.10 fb^{-1} collected by the CLEO-II detector [7] at the $\Upsilon(4S)$ resonance (referred to as ‘on-resonance’) and 1.60 fb^{-1} at a center-of-mass energy just below the threshold for production of $B\overline{B}$ pairs (referred to as ‘off-resonance’). The on-resonance data corresponds to 3.27×10^6 $B\overline{B}$ pairs. The off-resonance data is used to model the background from non- $B\overline{B}$ decays. Hadronic events are selected by requiring a minimum of three charged tracks, a total visible energy greater than 15% of the center-of-mass energy, and a primary vertex within ± 5 cm in the z direction and ± 5 mm in the $r - \phi$ plane from the nominal collision point.

The CLEO II detector measures both charged and neutral particles with excellent resolution and efficiency. Charged particles are measured in a 1.5 Tesla magnetic field through three nested cylindrical drift chambers covering 94% of the solid angle. These chambers are followed by time-of-flight (TOF) counters. Hadronic particle identification is accomplished by combining specific ionization (dE/dx) information from the drift chambers with TOF information. A CsI calorimeter provides excellent resolution for the reconstruction of photons. Information from the electromagnetic calorimeter and from the muon chambers are used to help reject electrons and muons as π candidates.

All candidate charged pions are required to be consistent with being produced at the primary event vertex. In addition, we use only charged tracks with $|\cos \theta| < 0.91$ with respect to the beamline, ensuring that they pass through all of the central drift chambers described above.

Isolated photons are paired to form π^0 candidates. Combinations that lie within 2.5 stan-

dard deviations of the nominal π^0 mass (about 12.5 MeV/c) are accepted as π^0 candidates. The photon momentum vectors are then kinematically constrained to the nominal π^0 mass.

When available, the dE/dX and TOF information for π_f candidates must each be consistent with the pion hypothesis to within three standard deviations. In addition, $\pi_f^-\pi_s^+$ candidates are required to have opposite charges.

Some events contain more than one slow pion that satisfies all requirements. In signal Monte Carlo, 5% (24%) of $\pi_f^-\pi_s^+$ ($\pi_f^-\pi_s^0$) events have more than one possible slow charged (neutral) pion. In $\pi_f^-\pi_s^0$ events, we select the neutral pion whose mass is closest to the nominal π^0 mass and in $\pi_f^-\pi_s^+$ events the charged pion with the smallest value of $(\cos \alpha - c)$ is selected.

The dominant source of background is from non- $B\bar{B}$ events. The distribution of decay products in these events tends to be jetlike while in $B\bar{B}$ events they tend to be uniformly distributed. To suppress non- $B\bar{B}$ events, each candidate event must satisfy $R_2 < 0.275$, where R_2 is the ratio of the second Fox-Wolfram moment to the zeroth moment [8], which tends to zero for uniformly distributed decay products. We also require that the events we use contain no charged track with momenta greater than 2.45 GeV. This requirement rejects a small fraction of non- $B\bar{B}$ events without rejecting any significant amount of signal.

To extract the branching fractions we perform a two-dimensional fit in $\cos \theta_B^*$ and $\cos \theta_{D^*}^*$, where the fit region is $|\cos \theta_B^*| < 1.65$ and $-1.6 < \cos \theta_{D^*}^* < 5.0$. The $\pi_f^-\pi_s^+$ and $\pi_f^-\pi_s^0$ data samples are fit simultaneously using the MINUIT [6] program. The fitting function combines contributions from the $B \rightarrow D^* \pi$ signal, other B decays and a fixed amount of non- $B\bar{B}$ background as described below.

The non- $B\bar{B}$ background shape and rate is determined from a sample of off-resonance data, that has been scaled for the relative luminosities between the on-resonance and off-resonance data samples. The $\cos \theta_B^*$ and $\cos \theta_{D^*}^*$ distributions in non- $B\bar{B}$ events are primarily determined by the π_f and π_s momentum spectrum in those events. Additionally, the shape is affected by the cone overlap requirement which has an acceptance that is dependent on $\cos \theta_B^*$ and $\cos \theta_{D^*}^*$. The acceptance is maximal when those two quantities are zero. This causes a peaking of the background around $\cos \theta_{D^*}^*$ equal to zero. Since the signal distribution is proportional to $\cos^2 \theta_{D^*}^*$, this background cannot fake the signal.

The B decay background is modeled using a large sample of simulated $B\bar{B}$ events. This background is dominated by modes that are kinematically able to produce a fast pion. The largest contributors are modes of the form $B \rightarrow D^{(\pm,0)}X$, where the X system is predominantly π , ρ or $\mu\nu_\mu$ and the $D^{(\pm,0)}$ can be in a higher spin state. The B decay background shape is similar to the non- $B\bar{B}$ background shape when each pion comes from a different B. However, when both pions come from the same B decay, the shape is more complicated. Typically, these decays will populate the region in and around the signal region, but none of them has the distinctive shape of the signal distribution. The branching fractions of these modes are allowed to vary in the fit in order to model the possible variations of the B decay background shape. The branching fractions of these modes are constrained by a Gaussian to the central value and error of the world average measurement as reported in the PDG [9], or left unconstrained if no measurement is available. They are also constrained to be the same in both the $\pi_f^-\pi_s^+$ and $\pi_f^-\pi_s^0$ samples.

One B decay background mode is handled differently. The Cabibbo-suppressed mode $B \rightarrow D^* K$ is indistinguishable in this analysis from $B \rightarrow D^* \pi$. However the ratio of branching

fractions, $\mathcal{B}(B \rightarrow D^* K)/\mathcal{B}(B \rightarrow D^* \pi)$, is predicted to be $(7.65 \pm 0.08\%)$ [9] from the ratio of CKM matrix elements and the ratio of decay constants. Therefore, a fixed fraction of signal events are subtracted off after correcting for the different acceptance for fast kaons versus fast pions.

The projections of the data and the fitting function in $\cos \theta_B^*$ and $\cos \theta_{D^*}^*$ are shown in Figure 1 for the $\pi_f^- \pi_s^+$ fit and in Figure 2 for the $\pi_f^- \pi_s^0$ fit. The sidebands outside the signal region are fitted well by the background functions. The sharp turn-on of signal at ± 1 can be seen while the background distribution in $\cos \theta_{D^*}^*$ shows the expected peaking in the signal region due to acceptance. The fitted number of signal events is given in Table I along with the product of acceptance and efficiency and the relevant D^* branching fraction. The background subtracted plots for the $\pi_f^- \pi_s^+$ and $\pi_f^- \pi_s^0$ fits for the $\cos \theta_{D^*}^*$ projection are shown in Figure 3. The peaks are asymmetric because the acceptance functions for charged and neutral slow pions have different momentum dependences.

The systematic uncertainty was determined to be 7.5% for $\overline{B}^0 \rightarrow D^{*+} \pi^-$ and 8.3% for $B^- \rightarrow D^{*0} \pi^-$. The error is dominated by uncertainties in the slow pion reconstruction efficiency, B decay background shape and simulation of the R_2 requirement. Additional errors come from the uncertainty in the number of $B\overline{B}$ pairs produced, signal shape smearing, Monte Carlo statistics and the simulation of $\cos \alpha$.

When converting from fitted yields to branching fractions we use the value of 3.27×10^6 $B\overline{B}$ pairs produced and assume that the ratio of $B^+ B^-$ to $B\overline{B}$ production (f_{+-}/f_{00}) times the ratio of lifetimes (τ_{B^\pm}/τ_{B^0}) is one. This is in agreement with the current CLEO measurement of $f_{+-} \tau_{B^\pm}/f_{00} \tau_{B^0} = 1.15 \pm 0.17 \pm 0.06$ [10]. We find:

$$\mathcal{B}(\overline{B}^0 \rightarrow D^{*+} \pi^-) = (2.81 \pm 0.11 \pm 0.21 \pm 0.05) \times 10^{-3} \quad (1)$$

$$\mathcal{B}(B^- \rightarrow D^{*0} \pi^-) = (4.34 \pm 0.33 \pm 0.34 \pm 0.18) \times 10^{-3} \quad (2)$$

where the first error is statistical, the second is systematics, and the third comes from the uncertainty in the $D^* \rightarrow D\pi$ branching fractions.

When taking the ratio of charged to neutral branching fractions, the systematic uncertainties due to the number of $B\overline{B}$ events, the R_2 requirement, and the fast pion reconstruction cancel. The ratio is measured to be $1.55 \pm 0.14 \pm 0.15$. The BSW model [11] predicts that the ratio is equal to $(1 + 1.29 a_2/a_1)$; this implies a value of a_2/a_1 of $0.19 \pm 0.04 \pm 0.05$.

These results agree with previous CLEO results [3] using full reconstruction and can be combined statistically with them as they have only a small fraction of events in common.

We also searched for the suppressed modes which produce a fast neutral pion. No signal was observed but the fit shape was in good agreement with the data, especially for the doubly CKM-suppressed decay which is expected to be entirely background.

We gratefully acknowledge the effort of the CESR staff in providing us with excellent luminosity and running conditions. This work was supported by the National Science Foundation, the U.S. Department of Energy, the Heisenberg Foundation, the Alexander von Humboldt Stiftung, Research Corporation, the Natural Sciences and Engineering Research Council of Canada, and the A.P. Sloan Foundation.

REFERENCES

- [1] J. Bjorken, Nucl. Phys. B (proc. Suppl.) **11** (1989) 325.
- [2] M. Bauer, B. Stech, and M. wirbel, Z. Phys. C **29** (1985) 637.
- [3] CLEO Collab., M.S. Alam *et al.*, Phys. Rev. D **50** (1994) 43.
- [4] ARGUS Collab., Ehrlichmann *et al.*, ZPhys. C **48** (1990) 543.
- [5] CLEO Collab., R. Giles *et al.*, Phys. Rev. D **30** (1984) 2279.
- [6] I. Brock, A fitting and Plotting Package Using MINUIT, CLEO/CSN Note 245-B, Revised (1992); F. James, MINUIT, Function Minimization and Error Analysis, CERN Program Library Long Writeup D506, Mar. 1994.
- [7] CLEO Collab., Y. Kubota *et al.*, Nucl. Instr. and Meth. **A320** (1992) 66.
- [8] G.C. Fox and S. Wolfram, Phys. Rev. Lett. **41** (1978) 1581.
- [9] L. Montanet *et al.*, Phys. Rev. D **50** (1994) 1173 and 1995 off year partial update for the 1996 edition (URL: <http://pdg.lbl.gov/>).
- [10] CLEO collab., C.S. Jessop *et al.*, CLNS 96/1455
- [11] M. Neubert, V. Rieckert, Q. P. Xu and B. Stech in *Heavy Flavours*, edited by A. J. Buras and H. Linder (World Scientific, Singapore, 1992).

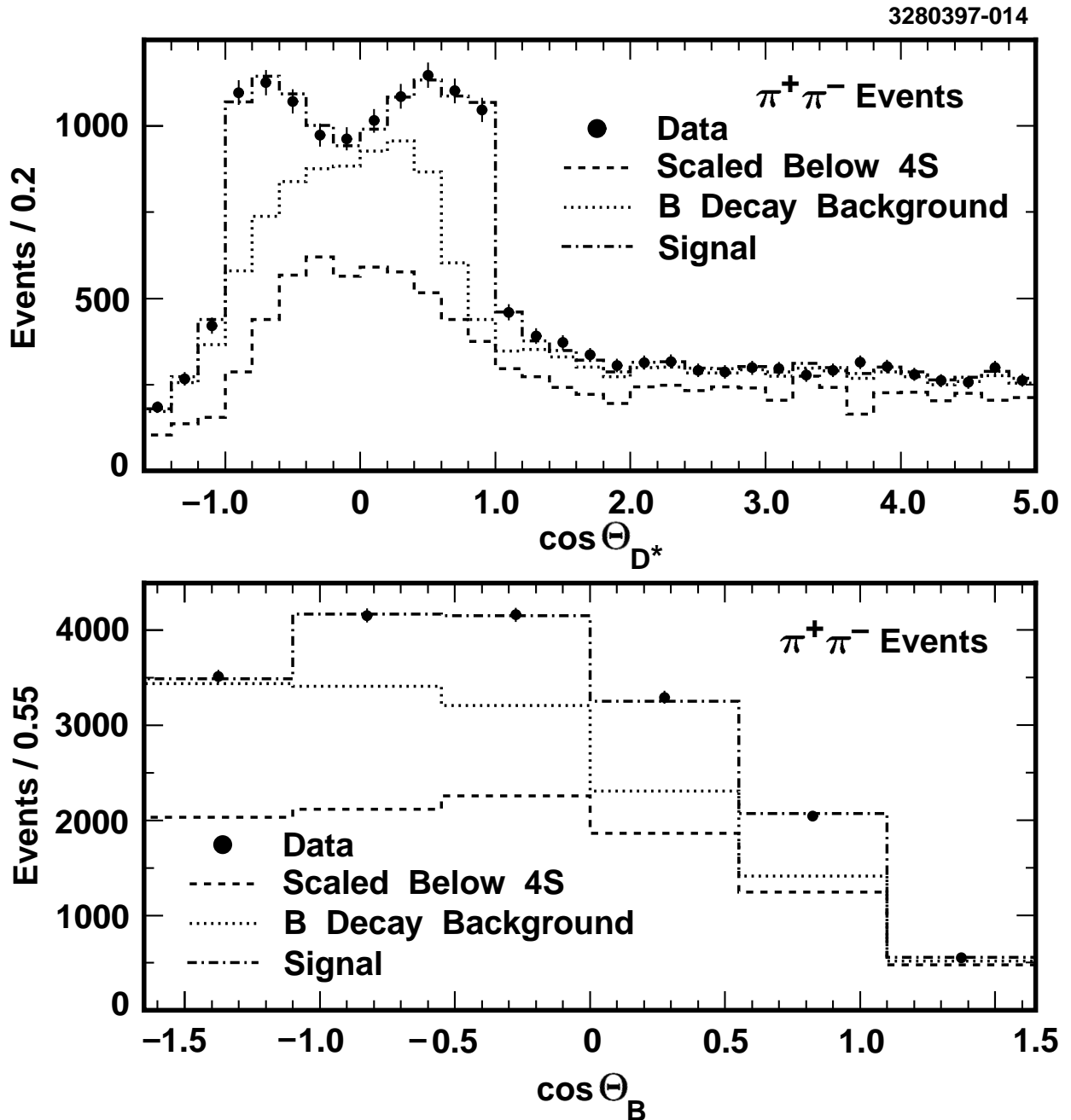


FIG. 1. The projections of the data histogram in $\cos \theta_B^*$ and $\cos \theta_{D^*}^*$ with the fitting function for the $\pi_f^- \pi_s^+$ fit.

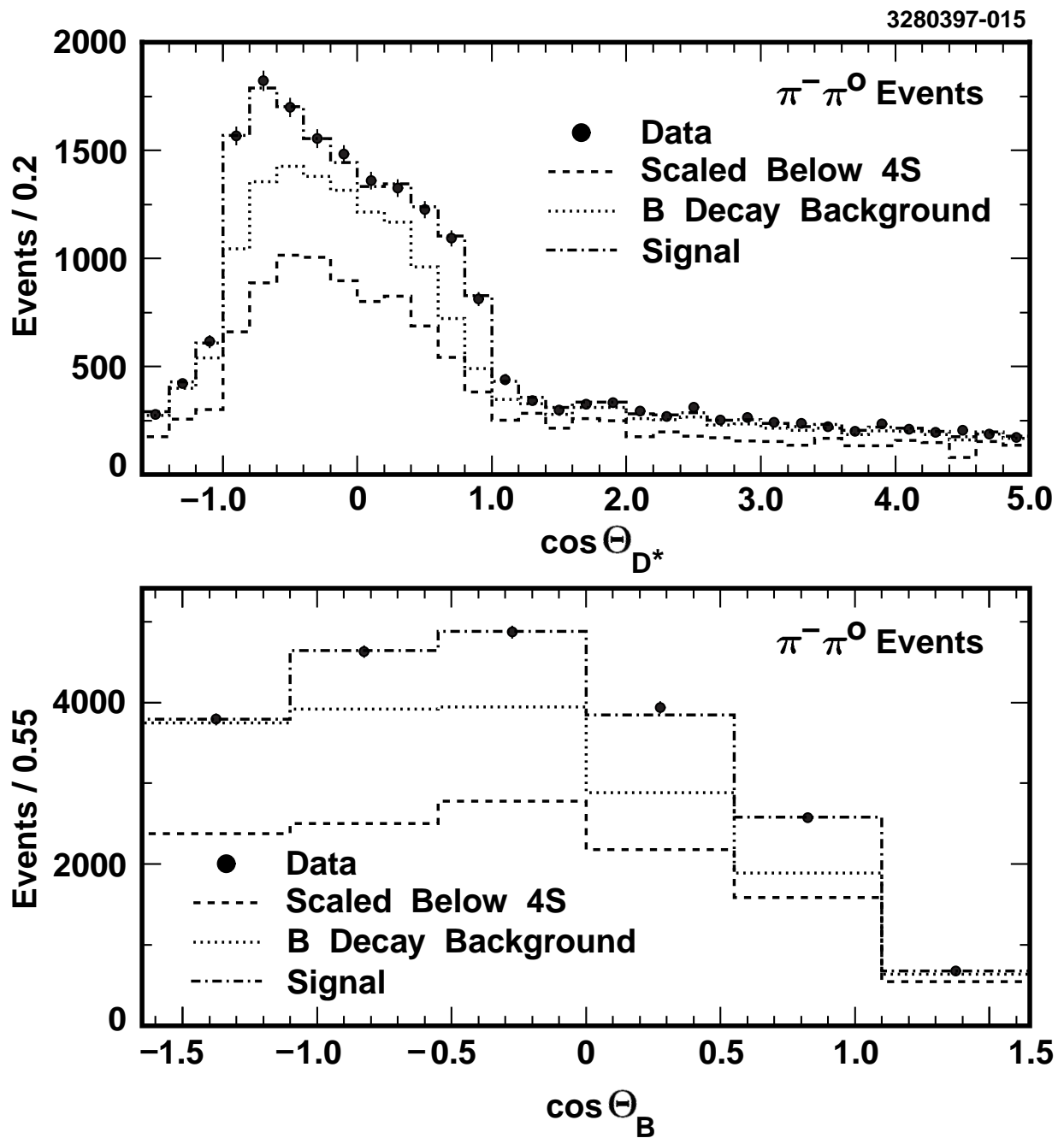


FIG. 2. The projections of the data histogram in $\cos \theta_B^*$ and $\cos \theta_{D^*}$ with the fitting function for the $\pi_f^- \pi_s^0$ fit.

TABLE I. The yield of signal events from the fits. The D^* branching fractions are not included in the calculation of acceptance times efficiency.

Mode	yield	acc \times eff	$\mathcal{B}(D^* \rightarrow D\pi)$
$\bar{B}^0 \rightarrow D^{*+}\pi^-; D^{*+} \rightarrow D^0\pi^+$	2612 ± 102	0.42	68.3%
$\bar{B}^0 \rightarrow D^{*+}\pi^-; D^{*+} \rightarrow D^+\pi^0$	513 ± 21	0.18	30.6%
$B^- \rightarrow D^{*0}\pi^-; D^{*0} \rightarrow D^0\pi^0$	1560 ± 115	0.18	61.9%

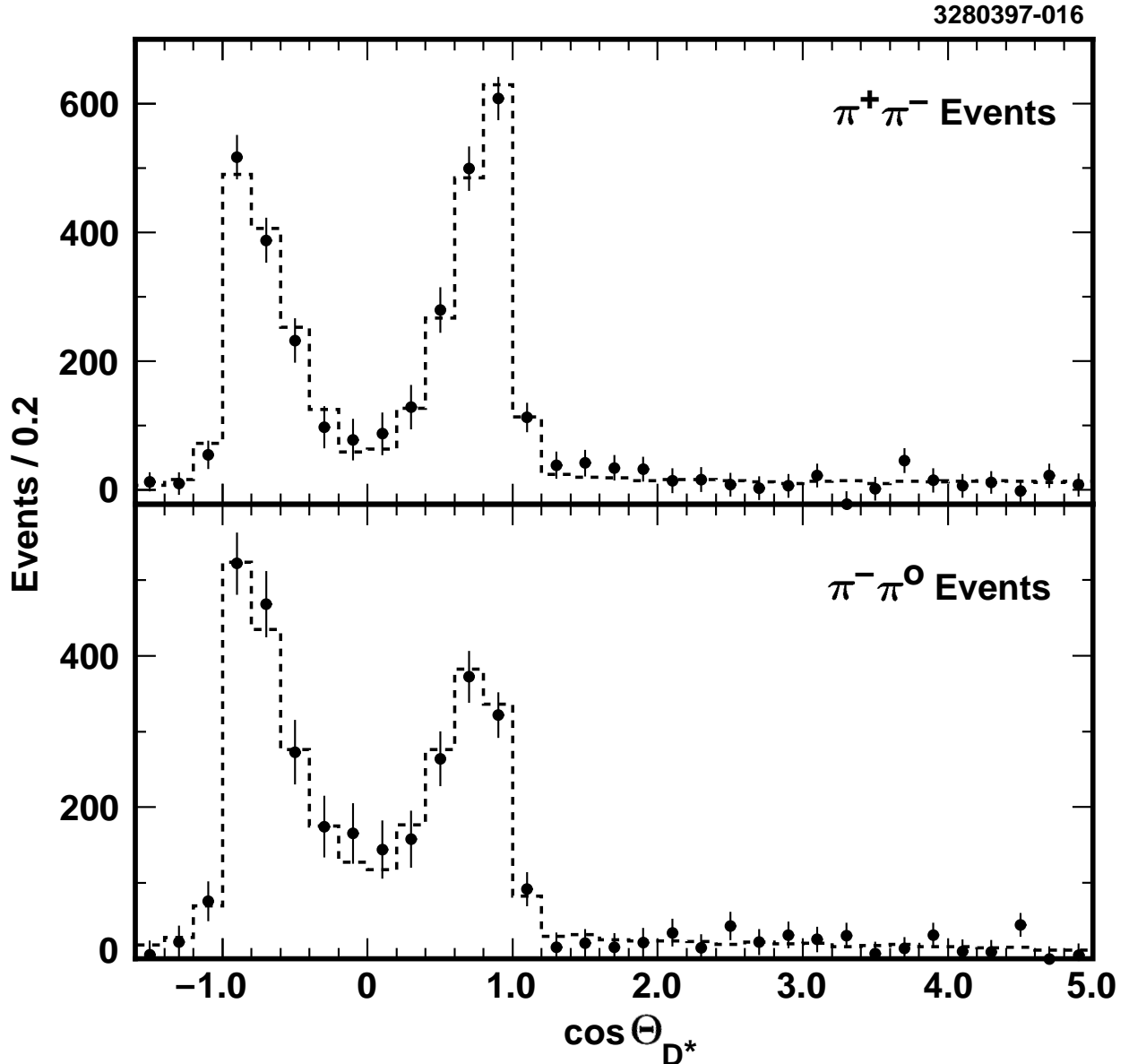


FIG. 3. The background subtracted projections of the data histogram in $\cos \theta_{D^*}$ for the $\pi_f^- \pi_s^+$ and $\pi_f^- \pi_s^0$ fits. The dashed line is the signal shape.